Bi-allelic variants in the ER quality-control mannosidase gene EDEM3 cause a congenital disorder of glycosylation

Daniel L Polla, Andrew C Edmondson, Sandrine Duvet, Michael E March, Ana Berta Sousa, Anna Lehman, Dmitriy Niyazov, Fleur van Dijk, Serwet Demirdas, Marjon A van Slegtenhorst, et al.

▶ **To cite this version:**

Daniel L Polla, Andrew C Edmondson, Sandrine Duvet, Michael E March, Ana Berta Sousa, et al.. Bi-allelic variants in the ER quality-control mannosidase gene EDEM3 cause a congenital disorder of glycosylation. American Journal of Human Genetics, 2021, 108 (7), pp.1342-1349. 10.1016/j.ajhg.2021.05.010 . hal-04470876

HAL Id: hal-04470876
https://hal.science/hal-04470876

Submitted on 21 Feb 2024

HAL is a multi-disciplinary open access archive for the deposit and dissemination of scientific research documents, whether they are published or not. The documents may come from teaching and research institutions in France or abroad, or from public or private research centers.

L'archive ouverte pluridisciplinaire **HAL**, est destinée au dépôt et à la diffusion de documents scientifiques de niveau recherche, publiés ou non, émanant des établissements d'enseignement et de recherche français ou étrangers, des laboratoires publics ou privés.

Biallelic variants in the ER quality control mannosidase gene *EDEM3* cause a congenital disorder of glycosylation comprising non-specific intellectual disability

Daniel L. Polla[1,2,22], Andrew C. Edmondson[3,22], Sandrine Duvet[4], Michael E. March[5], Ana Berta Sousa[6,7], Anna Lehman on behalf of CAUSES Study[8], Dmitriy Niyazov[9], Fleur van Dijk[10], Serwet Demirdas[11], Marjon A. van Slegtenhorst[11], Anneke J.A. Kievit[11], Celine Schulz[4], Linlea Armstrong[8], Xin Bi[12], Daniel J. Rader[5,12,13], Kosuke Izumi[3], Elaine H. Zackai[3], Elisa de Franco[14], Paula Jorge[15,16], Sophie C. Huffels[14], Sian Ellard[14,17], Dirk J. Lefeber[18,19], Avni Santani[20,21], Nicholas J. Hand[13,22], Hans van Bokhoven[1,22], Miao He[21,22,*], Arjan P.M. de Brouwer[1,22,*]

[1] Department of Human Genetics, Donders Institute for Brain, Cognition and Behavior, Radboud University Medical Center, 6500 HB Nijmegen, The Netherlands.

[2] CAPES Foundation, Ministry of Education of Brazil, Brasília, Brazil

[3] Department of Pediatrics, Division of Human Genetics, Children's Hospital of Philadelphia, 19104 Philadelphia, PA, USA

[4] Univ. Lille, CNRS, UMR 8576 – UGSF – Unité de Glycobiologie Structurale et Fonctionnelle, F-59000 Lille, France

[5] Center for Applied Genomics, Children's Hospital of Philadelphia, 19104 Philadelphia, PA, USA

[6] Serviço de Genética Médica, Hospital de Santa Maria, Centro Hospitalar Universitário Lisboa Norte, 649-035 Lisboa, Portugal

[7] Faculdade de Medicina da Universidade de Lisboa, 1649-028 Lisboa, Portugal

[8] Department of Medical Genetics, University of British Columbia, V6H 3N1 Vancouver, BC, Canada

[9] Tulane School of Medicine, University of Queensland, 1315 Jefferson Highway, 70121 New Orleans, LA

[10] North West Thames Regional Genetics Service, London North West University Healthcare NHS Trust, Watford Road, Harrow, HA1 3UJ London, UK

[11] Department of Clinical Genetics, Erasmus University Medical Center, 3015 Rotterdam, The Netherlands

[12] Department of Medicine, Perelman School of Medicine, University of Pennsylvania, 19104 Philadelphia, PA, USA

[13] Department of Genetics, Perelman School of Medicine, University of Pennsylvania, 19104 Philadelphia, PA, USA

[14] Department of Molecular Genetics, Royal Devon & Exeter NHS Foundation Trust, Barrack Road, EX2 5DW Exeter, UK

entro de Genética Médica Jacinto de Magalhães (CGMJM), Centro Hospitalar do Porto, CHP, E.P.E., 4099-028 Porto, Portugal

nit for Multidisciplinary Research in Biomedicine, Abel Salazar Institute of Biomedical Sciences, University of Porto, 4099-028 Porto, Portugal

[17] College of Medicine and Health, University of Exeter, Barrack Road, EX2 5DW Exeter, UK

[18] Department of Neurology, Donders Institute for Brain, Cognition, and Behavior, Radboud University Medical Center, 6525 GA Nijmegen, The Netherlands

[19] Department of Laboratory Medicine, Translational Metabolic Laboratory, Radboud University Medical Center, 6525 GA Nijmegen, The Netherlands

[20] Department of Pathology and Laboratory Medicine, Children's Hospital of Philadelphia, 19104 Philadelphia, PA, USA

[21] Department of Pathology and Laboratory Medicine, Perelman School of Medicine, University of Pennsylvania, 19104 Philadelphia, PA, USA

[22] These authors contributed equally to this work.

* Correspondence to:

Miao He

HeM@email.chop.edu

Arjan P. M. de Brouwer

Arjan.debrouwer@radboudumc.nl

Abstract

EDEM3 encodes a protein that converts $Man_8GlcNAc_2$ isomer B to $Man_{7\text{-}5}GlcNAc_2$. It is involved in the endoplasmic reticulum-associated degradation pathway, responsible for the recognition of misfolded proteins that will be targeted and translocated to the cytosol and degraded by the proteasome. In this study, through a combination of exome sequencing and gene matching, we have identified 11 individuals from six independent families with biallelic protein truncating variants and one family with a compound heterozygous missense variant in *EDEM3*. The affected individuals present with a novel inherited congenital disorder of glycosylation (CDG) consisting of neurodevelopmental delay and variable facial dysmorphisms. Experiments in human fibroblast cell lines, human plasma, and mouse plasma and brain tissue, demonstrated decreased trimming of $Man_8GlcNAc_2$ isomer B to $Man_7GlcNAc_2$, consistent with loss of EDEM3 enzymatic activity. In human cells, $Man_5GlcNAc_2$ to $Man_4GlcNAc_2$ conversion is also diminished with an increase of $Glc_1Man_5GlcNAc_2$. Furthermore, analysis of the unfolded protein response showed a reduced increase in *PERK* expression upon stimulation with tunicamycin as compared to controls, suggesting an impaired unfolded protein response. The aberrant plasma N-glycan profile in patients provides a quick, clinically available test for validating variants of uncertain significance that may be identified by molecular genetic testing. We propose to call this deficiency EDEM3-CDG.

Main Text

The endoplasmic reticulum-associated degradation (ERAD) pathway recognizes misfolded proteins that will be targeted and translocated to the cytosol and degraded by the proteasome [1–4]. The best characterized system is dedicated to N-linked glycoproteins, the glycoprotein ERAD (gpERAD) pathway. Proteins that fail to fold or assemble properly are subjected to degradation via specific trimming of high-mannose-type glycans in the lumen of the ER [5,6]. In mammals, EDEM2 and ERmanI are known to primarily catalyze the first step, conversion of $Man_9GlcNAc_2$ (M9) to $Man_8GlcNAc_2$ isomer B (M8B) [1–3]. EDEM3 and EDEM1 are further involved in catalyzing the second step, the conversion of M8B to $Man_7GlcNAc_2$ (M7) [7–12]. These products are then recognized by lectin OS-9 in the ER lumen and targeted for degradation in the cytosol [13].

Cells can degrade misfolded proteins from the secretory pathway using both the glycan-dependent and glycan-independent ERAD pathways [14–16]. The presence of misfolded ER proteins is harmful to cells and is involved in several congenital disorders of glycosylation (CDG) [17–20], such as PMM2-CDG (OMIM 212065), MPI-CDG (OMIM 602579), ALG6-CDG (OMIM 603147), DPM1-CDG (OMIM 608799), ALG12-CDG (OMIM 607143), and DPAGT1-CDG (OMIM 608093). If this degradative process fails to effectively remove misfolded and abnormal proteins from the ER, then the unfolded protein response (UPR) is initiated [1–4]. UPR is critical to maintain cellular homeostasis. In mammals, three classical ER stress markers are known to reflect induction of the UPR: protein kinase RNA-like endoplasmic reticulum kinase (PERK), activating transcription factor 6 (ATF6) and inositol requiring enzyme 1 (IRE1) [21,22]. Upon protein overload in the ER, UPR signaling via the PERK, ATF6, and IRE1 pathways is activated to increase ER capacity, inhibit translation, and stimulate the removal of excess and misfolded proteins [23–26]. Persistent activation of UPR can lead to apoptosis [27–29].

Here, we describe 11 individuals from six independent families with biallelic protein truncating variants and one additional individual with a compound heterozygous missense variant in *EDEM3* (OMIM 610214) identified by exome sequencing (**Fig. 1**) and collected

through GeneMatcher [30]. The parents or legal guardians provided written informed consent. All relevant approvals from the institutional ethics committees of the participating institutions were obtained. In patients from families 1 and 2, a biallelic frameshift deletion, c.1859del, p.(Ile620Thrfs*7), was identified in *EDEM3* (GenBank: NM_025191.3; **Fig. 1**). Additionally, two frameshift variants, c.2001dupA, p.(Ala668Serfs*9) and c.1369delA, p.(Arg457Glufs*28), were identified in family 3. In family 4, a biallelic nonsense variant, c.940A>T, p.(Arg314*), was found, resulting from maternal uniparental isodisomy of chromosome 1. In family 5, a canonical splice site donor variant c.853+1G>T and a nonsense variant c.1407 T>A, p.(Tyr469*) was identified and, in family 6, a biallelic frameshift deletion c.1382_1385del, p.(Phe461Serfs*23). Finally, in family 7, the compound heterozygous changes c.182A>G, p.(Asp61Gly), and c.1366G>A, p.(Asp456Asn), were identified. Sanger sequencing showed that the patients were either homozygous or compound heterozygous for the identified *EDEM3* variants. The unaffected parents were all heterozygous carriers. The p.(Asp61Gly) missense variant was found in six heterozygous individuals, out of 218,508 alleles, in GnomAD (https://gnomad.broadinstitute.org; rs777353823) and predicted to be 'disease-causing' by Mutation Taster[31], but 'tolerated' by SIFT[32]. The p.(Asp456Asn) missense variant was not present in GnomAD and predicted to be 'disease-causing' by both Mutation Taster and SIFT. Both are present in the so-called 'Glyco_Hydro_47 domain', which is essential for the α-mannosidase activity of the protein.

Affected individuals from family 1 and 2 have the identical c.1859del (p.(Ile620Thrfs*7)) *EDEM3* variant, but there are no records of inter-familial consanguinity in these families. Comparison of the exome data from two affected individual from family 1 and from one affected individual from family 2, indicated that these three individuals carried a common identical region of homozygosity of 3.16 Mb (Chr1: 182993025-186157274, Hg19) surrounding *EDEM3*. In addition, this variant was looked for in 96 healthy controls in the Romani population in Portugal, among whom one heterozygous allele was detected. Since families 1 and 2 are of Portuguese Romani origin, this suggests a possible founder effect.

All affected individuals presented with developmental delay and/or intellectual disability (ID) and speech delay (**Supplemental Table S1**). Hypotonia was present in six out of 12 patients. Dysmorphic facial features, such as narrow palpebral fissures (6/12), epicanthal folds (6/12), increased nasal height (8/12), bulbous nasal tip (6/12), hypoplastic alae nasi (9/12), short philtrum (6/12), thin upper lip (9/12) and retrognathia (6/12) were also found in half or more of the patients. Additionally, gastro-esophageal reflux was observed in three patients, and two individuals had early feeding difficulties, requiring a nasogastric tube and of these one individual needed a percutaneous endoscopic gastrostomy placement. Brain magnetic resonance imaging (MRI) of affected individuals from families 2, 3, and 5 did not detect structural abnormalities or myelination defects.

The protein truncating variants identified in this study are expected to result in reduced protein expression, due to degradation of mRNA via nonsense mediated decay (NMD), and in a truncated protein [33,34]. Accordingly, quantitative real time PCR (qPCR) analysis showed that *EDEM3* mRNA levels in EBV-LCLs from patients in family 1 were significantly decreased to 17% as compared to healthy controls (P=0.0078; **Fig. 2A**) and could be rescued with cycloheximide (CHX), an inhibitor of NMD, suggesting that the biallelic c.1859del frameshift variant triggers NMD. We repeated these experiments in fibroblasts from patients in families 1 and 3 and confirmed that *EDEM3* is degraded to 18% of normal levels by NMD (P=0.0015; **Fig. 2B**). As the function of EDEM3 could theoretically be compensated by EDEM1[35], we quantified *EDEM1* (OMIM 607673) RNA levels in patient and control fibroblast cell lines. *EDEM1* levels were at 97% of normal levels (P=0.9373) in fibroblast patient cell lines (**Fig. 2C**). The comparative levels of *EDEM1* in patient and control fibroblast cell lines seems to suggest that *EDEM1* expression does not compensate for the reduction of *EDEM3* in these cells.

Previous studies have shown that EDEM3 belongs to a group of proteins that accelerate the degradation of misfolded glycoproteins in the ER. It is one of the ER 1,2-alpha mannosidases, and specifically trims M8B to M7 (**Fig. 3A**), which is then recognized by lectin OS-9 and targeted for degradation [7,8,10,11]. We hypothesized that loss of M8B to M7 trimming

activity would result in accumulation of abnormal N-glycans. Therefore, we determined the N-glycan profiles of total cellular glycoproteins prepared from a control and a patient-derived fibroblast cell line. Total N-glycan analysis using mass spectrometry in the patient's fibroblast cell line showed accumulation of M9 and M8B and reduced M7 isomer A and $Man_6GlcNAc_2$ (M6) levels (**Fig. S1**). To study more precisely the impact of EDEM3 deficiency, we also analyzed the N-glycan profile after a pulse-chase experiment using [2-3H] mannose as precursor. We tested whether the variants in *EDEM3* affect the level of glycoproteins in fibroblast cell lines of individuals from families 1 and 3. In control fibroblast cells, we observed the anticipated levels of M8, M9 and $Glc_1Man_9GlcNAc_2$ (G1M9; **Fig. 3B**). EDEM3 deficient patient cells from patients of family 1 and 3 exhibited a similar pattern of N-glycan structures. However, after 2h of chase, the peaks for M7 and M6 did not appear in the patient's cells (**Fig. 3B**), indicating that the 1,2-alpha mannose residues were not removed from the M8B N-glycans during the chase consistent with absence of the physiological function of EDEM3 (**Fig. 3A**). In addition, appearance of smaller structures $Glc_1Man_5GlcNAc_2$ (G1M5) and $Man_5GlcNAc_2$ (M5) was observed in EDEM3 deficient patients cell lines. The structural characterization of these two species have been checked by using either saitoi or jack bean alpha-mannosidase treatments (see Supplemental data S2a-b). We speculate that M5 is also transferred onto newly synthesized proteins and would be reglucosylated by the UDP-Glc : glycoprotein glucosyltransferase during calnexin cycle (**Fig. 3A**).(Ref 39)

To evaluate the N-glycosylation of secreted glycoproteins, we studied the N-glycan profile of total plasma glycoproteins from all patients including the one with the compound heterozygous missense variants, using our recently described and clinically validated semi-quantitative N-glycan assay [36]. The N-glycan profiles from patients showed decreased levels of low mannose N-glycan species M3-M7 (**Fig. 3C**) with preserved normal or sometimes mildly increased abundance of M8 and M9 as compared to control subjects. Ratios of the N-glycan abundances were also explored and patients had prominently decreased ratios of M5/M9, M6/M9, and M7/M9 as well as decreased M3/M4 (**Fig. 3D**; **Supplemental Table S2**). M6/M9 ratio provided the highest discrimination between tested obligate heterozygotes

(parents, n=4) and affected individuals (n=12; **Supplemental Table S3**). In theory, M3 can be produced by multiple pathways with or without EDEM3, thus we used M9/M3 ratio to normalize M9 abundance. M9/M3 was increased in all 12 patients. Stepwise ratio analysis for plasma N-linked polymannose species showed a reduction of M7/M8 that is significant in patients, consistent with EDEM3 being the key enzyme in trimming M8B to M7 (**Supplemental Table S3**) [7,11]. Of note, human transferrin was normally glycolated in the common clinical screening test for CDG in the three patients from family 3.

N-glycan profiles were also obtained from *Edem3* knockout (KO) mice (**Fig. S3**). Although *Edem3* knockout mice did not present with any obvious phenotype, subtle changes have been noted, such as reduced weight of brains and body, and largely skewed ratios of homozygous knockout pups versus heterozygous and wild type pups. The profiles were acquired using a previously described method [36]. Similar to human patients, plasma from mice showed decreased ratios of M5/M9, M6/M9, and M7/M9 (P<0.02; **Fig. S4B**). In addition, mouse plasma proteins had significantly increased abundance of M8 and M9 (P<0.01; **Fig. S4A**). We also assayed mouse brain lysate for N-glycan profiles (**Fig. S4C**) and ratios (**Fig. S4D**). While plasma N-glycans reflect glycosylation of mature secreted glycoproteins and glycopeptides, N-glycan profiling of mouse tissue also includes cellular glycoproteins. Similar to mouse plasma N-glycan profiling, mouse brain showed increased high-mannose M8 and M9 N-glycan species (**Fig. S4C**) and decreased ratios of M5/M9 and M6/M9 (**Fig. S4D**).

N-glycan analysis of both *Edem3* KO mouse brain and plasma showed significant increases of the abundance M8 and M9. In human, not all the EDEM3 patients have increased M8 or M9 in the plasma. Instead, M9/M3 ratio is increased in all 12 patients. Thus, the known function of EDEM3 in trimming M8B is likely shared by both human and mice. The M9/M3 ratio serves a more sensitive diagnostic biomarker than M8 or M9 abudance in plasma. N-linked M3 and M4 are newly discovered small high-mannose species with low abundance on normal plasma glycoproteins including transferrin [36]. Increases of M3 and M4 abundances have been reported as important diagnostic biomarkers for type I CDG subtypes

including PMM2-CDG, MPI-CDG, ALG3-CDG and ALG9-CDG [36–38]. Significantly reduced abundance of N-linked M3 with a decreased M3/M4 ratio (P<0.0001), however, has not been reported before. The reduction of M3 in all the patients suggests that a large portion of N-linked M3 in the normal population is probably derived from glycan trimming involving human EDEM3 (**Fig. 3A**). In the plasma from *Edem3* KO mouse, M3/M4 ratio is not increased (**Fig. S4B,D**). Instead of increased M7/M8 ratio in human, the increased M6/M7 ratio is the most significant, which may reflect a difference in overall substrate specificity between human and mouse EDEM3. The glycosylation abnormalities in both cellular or tissue proteins and secreted mature proteins indicate a global impact on protein N-glycosylation in EDEM3 deficiency. Consistent with our findings, it was previously demonstrated that EDEM3 participates in mannose trimming from total glycoproteins and not just misfolded proteins for ERAD [7]. Therefore, we propose this deficiency to be a novel CDG, EDEM3-CDG.

The finding of abnormal N-glycan profiling pattern with reduced M3/M4, M5/M9, M6/M9 and M7/M9 ratios, and increased M9/M3 among EDEM3-CDG patients, provides additional diagnostic biomarkers for validating variants of uncertain significance, *i.e.* missense variants in *EDEM3*. One of the 12 EDEM3-CDG patients showed normal plasma of M5/M9 and M6/M9 ratios, but also showed the lowest plasma N-linked M3/M4 ratio at 0.27 (normal 0.39-0.56) and a significantly increased M9/M3 ratio at 3.30 (normal 1.16-2.92) in this cohort. Therefore, the combination of high M9/M3 and low M3/M4 ratios might also provide diagnostic clues for EDEM3-CDG when M5/M9 and M6/M9 ratios are normal.

G1M5 accumulation is a marker for impaired UPR [39]. Therefore, we tested whether UPR, a key quality-control machinery in the cell, which is activated in response to the accumulation of misfolded proteins [22], is affected in EDEM3-CDG. qPCR analysis of total mRNA from EBV-LCLs from patients showed decreased stimulation of *ERN1* (*IRE1*; OMIM 604033) and *IEF2AK3* (*PERK*; OMIM 604032) when cells were treated with tunicamycin, a stress-inducing compound, as compared to controls (**Fig. 2D**). *ATF6* (OMIM 605537) expression levels were similar. The difference in *IRE1* gene expression levels was not significant (P=0.091), whereas the decreased stimulation of *PERK* expression levels in

patient cell lines was significant (*P*=0.020; **Fig. 2E**), suggesting that UPR is affected in EDEM3-CDG or that patient cell lines have an increased capacity to eliminate misfolded proteins.

In conclusion, we show that biallelic *EDEM3* variants cause EDEM3-CDG, a novel CDG with non-specific developmental delay and/or intellectual disability. Several patients also have mild facial dysmorphisms. Given the increased accessibility of blood for clinical testing, quantitative N-glycan analysis provides additional diagnostic biomarkers for validating variants of uncertain significance that may be identified on molecular genetic testing. Further functional studies are necessary to determine the precise pathophysiological mechanism of this novel CDG.

Ackowledgments

We are grateful to the families that have participated to this study. This work was supported the EU FP7 Large-Scale Integrating Project Genetic and Epigenetic Networks in Cognitive Dysfunction (241995) (to HvB), by National Institutes of Health (NIH) grant 5R01GM115730-03 (to MH), U54 NS115198 (to ACE and MH) and T32GM008638 (to ACE), and the Transatlantic Network of Excellence grant (10CVD03) from the Fondation Leducq and NIH NHGRI U01HG006398 (to DJR). Family 4 was enrolled in the CAUSES Study; investigators include Shelin Adam, Christele Du Souich, Alison Elliott, Anna Lehman, Jill Mwenifumbo, Tanya Nelson, Clara Van Karnebeek, and Jan Friedman; it is funded by Mining for Miracles, British Columbia Children's Hospital Foundation (grant number F15-01355) and Genome British Columbia (grant number F16-02276). DLP is recipient of a CAPES Fellowship (99999.013311/2013-01). XB is supported by AHA career development award (19CDA34630032).

Figures

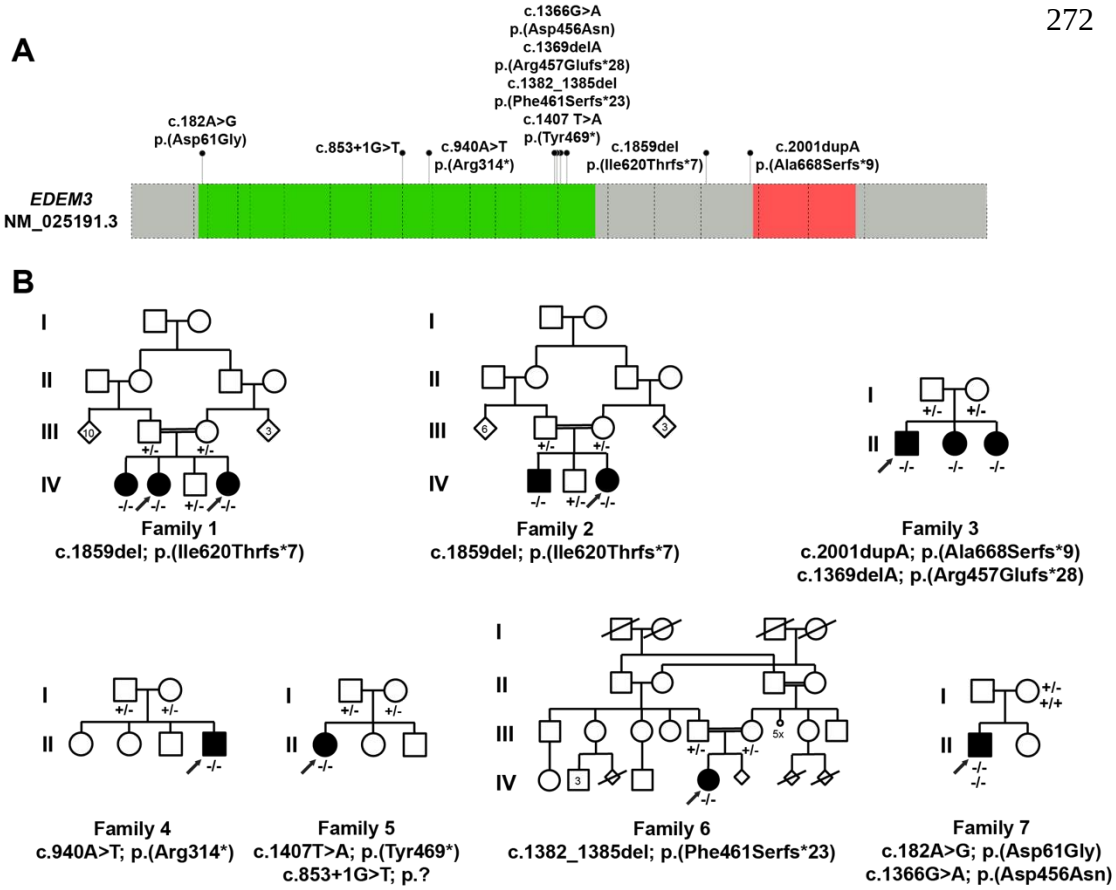
A
c.1366G>A
p.(Asp456Asn)
c.1369delA
p.(Arg457Glufs*28)
c.1382_1385del
p.(Phe461Serfs*23)
c.1407 T>A
p.(Tyr469*)
c.182A>G
p.(Asp61Gly)
c.853+1G>T
c.940A>T
p.(Arg314*)
c.1859del
p.(Ile620Thrfs*7)
c.2001dupA
p.(Ala668Serfs*9)
EDEM3
NM_025191.3
B
Family 1
c.1859del; p.(Ile620Thrfs*7)
Family 2
c.1859del; p.(Ile620Thrfs*7)
Family 3
c.2001dupA; p.(Ala668Serfs*9)
c.1369delA; p.(Arg457Glufs*28)
Family 4
c.940A>T; p.(Arg314*)
Family 5
c.1407T>A; p.(Tyr469*)
c.853+1G>T; p.?
Family 6
c.1382_1385del; p.(Phe461Serfs*23)
Family 7
c.182A>G; p.(Asp61Gly)
c.1366G>A; p.(Asp456Asn)
C
Family 1
IV-1
Age 18 years
IV-2
Age 12 years
IV-4
Age 6 years
Family 2
IV-1
Age 1 year
IV-3
Age 13 years
Family 3
II-1
Age 9 years
II-2
Age 8 years
II-3
Age 4 years
Family 5
II-1
Age 4 years
Family 6
IV-5
Age 18 months

Fig. 1. Biallelic variants in *EDEM3* lead to developmental delay or intellectual disabilities and dysmorphic features (A) Schematic representation of human EDEM3 including the positions and the predicted effect on protein level of the seven identified variants in this study. Green box represents the Glyco_Hydro_47 domain and the red box represents the PA domain. Dashed boxes represent exons. (B) Pedigrees of EDEM3-CDG families including the presence of the mutation. -: mutation present; +: wild type. (C) Craniofacial features of affected individuals including narrow palpebral fissures, epicanthal folds, increased nasal height, bulbous nasal tip, hypoplastic alae nasi, short philtrum, thin upper lip, and retrognathia.

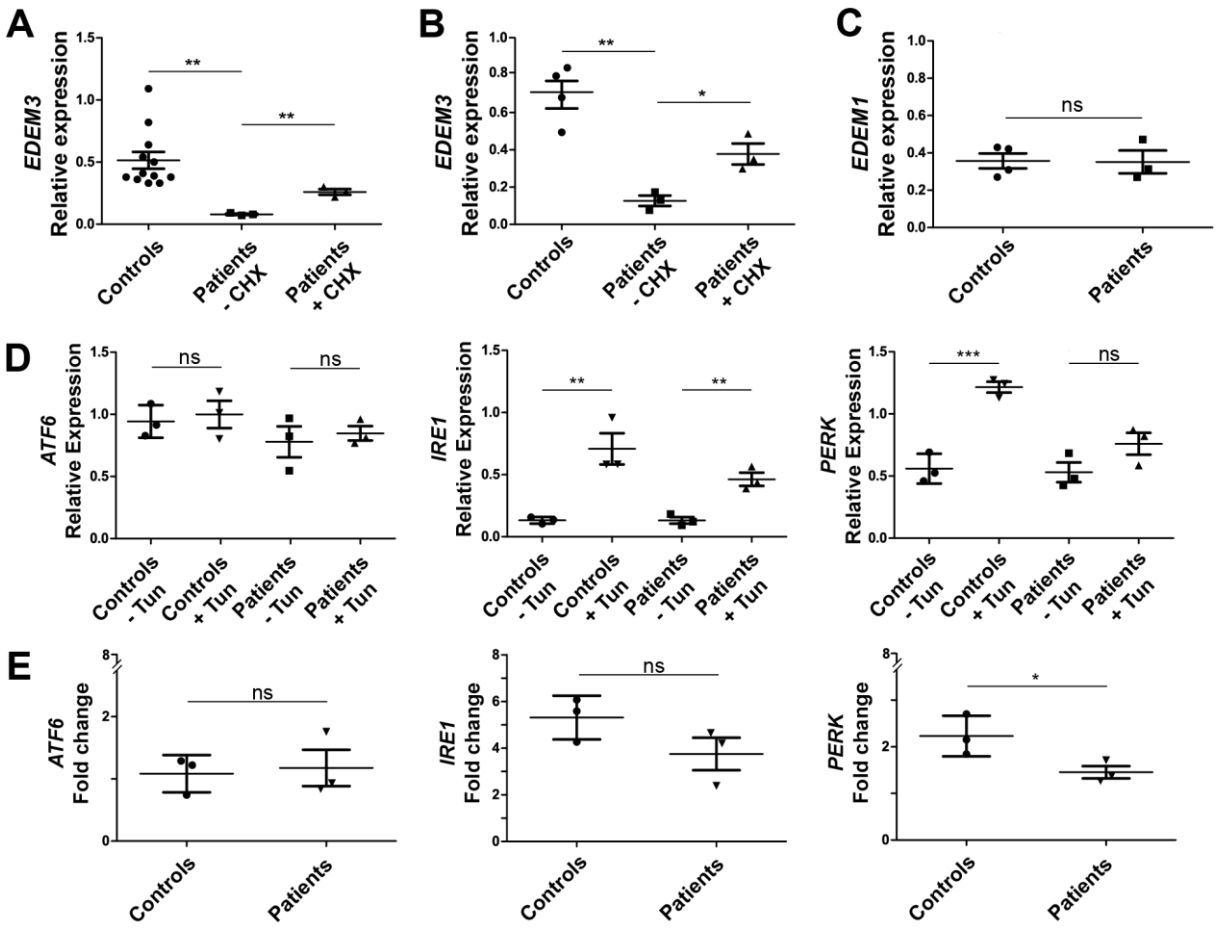

Fig. 2. Relative expression of *EDEM3* mRNA and expression analysis of UPR markers. (A) A significant decrease of mRNA levels is seen between relative expressions of *EDEM3* in EBV-LCL from three affected individuals of family 1 with the biallelic c.1859del frameshift variant (n=3) compared to healthy controls (n=12; *P*=0.0078) and samples treated with cycloheximide (CHX; *P*=0.0016; n=3), normalized according to three housekeeping genes. (B) *EDEM3* expression in fibroblast cell lines from family 1 (individual IV-4) and family 3 (individuals II-1 and II-2) confirming these results (*P*=0.0015 and *P*=0.0161 for CHX. Four controles were used. (C) *EDEM1* expression in fibroblast cell lines from family 1 (individual IV-4) and family 3 (individuals II-1 and II-2) showing normal expression levels (*P*=0.9373). Four controles were used. (D) Analysis of total mRNA from EBV-LCL cell lines from controls revealed increased mRNA expression after treatment with tunicamycin (Tun) of *IRE1* and *PERK* but not of *ATF6.* (E) Affected individuals' mRNA from family 1 showed significantly decreased induction of *PERK* expression when compared to controls (*P*=0.020), whereas *ATF6* and *IRE1* did not change significantly (*P*=0.423 and *P*=0.091, respectively). Experiments D and E were performed with three control cell lines and three patients cell lines. ns= not significant; *= *P*<0.05; ** *P*<0.01; *** *P*<0.001.

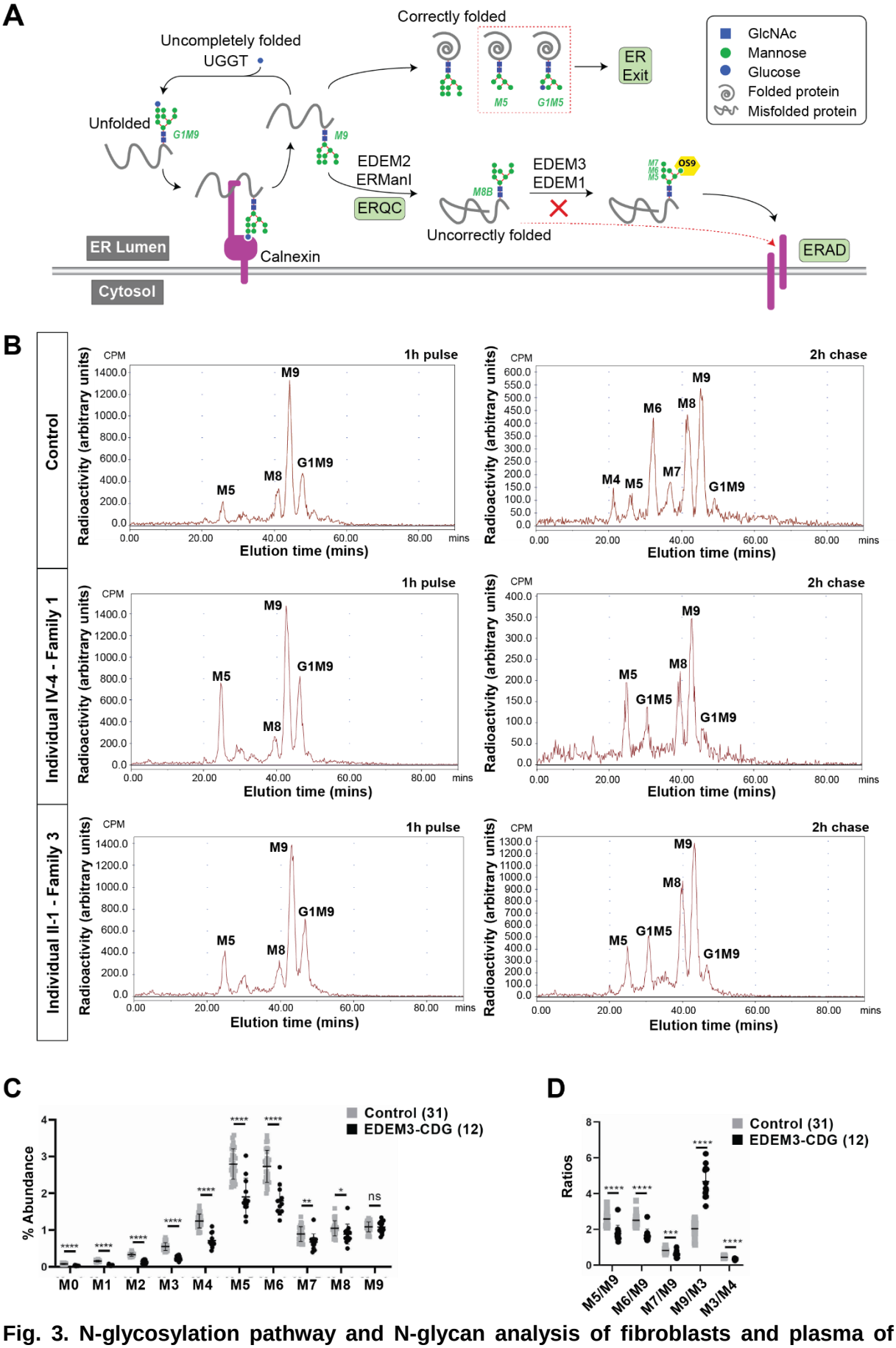

Fig. 3. N-glycosylation pathway and N-glycan analysis of fibroblasts and plasma of human subjects. (A) N-glycosylaton pathway and the role of EDEM proteins in the mannose

trimming and targeting for protein degradation in the cytosol. Red dashed lines show the accumulation of N-glycans in EDEM-CDG individuals. (B) Accumulation of G1M5 and M5 on newly synthesized N-glycoproteins in two EDEM3-CDG patient fibroblast cell lines. Patient fibroblasts from family 1 (individual IV-4) and family 3 (individual II-1) and one control were incubated with [2-3H] mannose for 1h and chased during 2h. (C) Percent abundance of N-glycan species obtained from EDEM3-CDG patients and controls. (D) Plot of ratio of N-glycan species. Bars indicate mean values. Error bars represent standard deviation. Indicated P-values from Student's T-test, ns = not significant; *P<0.05; **P<0.01; ***P<0.001; ****P<0.0001.

Supplemental data

Fig. S1. N-glycan analysis of fibroblasts.
Fig. S2. HPLC analysis of EDEM3 patient fibroblast N-glycans after jack bean α-mannosidase treatment.
Fig. S3. Deletion of 47bp in mouse Edem3 exon 3 results in a protein null.
Fig. S4. N-glycan analysis of Edem3 KO and WT mice.
Supplemental Table S1. Clinical data of EDEM3-CDG patients.
Supplemental Table S2. The abundance of plasma N-glycans in EDEM3-CDG patients.
Supplemental Table S3. Summary of high mannose changes in EDEM3-CDG patients.

References

Automatic citation updates are disabled. To see the bibliography, click Refresh in the Zotero tab.1. Brodsky, J.L. (2012). Cleaning Up: ER-Associated Degradation to the Rescue. Cell *151*, 1163–1167.

2. Needham, P.G., and Brodsky, J.L. (2013). How early studies on secreted and membrane protein quality control gave rise to the ER associated degradation (ERAD) pathway: the early history of ERAD. Biochim. Biophys. Acta *1833*, 2447–2457.

3. Smith, M.H., Ploegh, H.L., and Weissman, J.S. (2011). Road to ruin: targeting proteins for degradation in the endoplasmic reticulum. Science *334*, 1086–1090.

4. Thibault, G., and Ng, D.T.W. (2012). The endoplasmic reticulum-associated degradation pathways of budding yeast. Cold Spring Harb. Perspect. Biol. *4*,.

5. Aebi, M., Bernasconi, R., Clerc, S., and Molinari, M. (2010). N-glycan structures: recognition and processing in the ER. Trends Biochem. Sci. *35*, 74–82.

6. Molinari, M. (2007). N-glycan structure dictates extension of protein folding or onset of disposal. Nat. Chem. Biol. *3*, 313–320.

7. Hirao, K., Natsuka, Y., Tamura, T., Wada, I., Morito, D., Natsuka, S., Romero, P., Sleno, B., Tremblay, L.O., Herscovics, A., et al. (2006). EDEM3, a soluble EDEM homolog, enhances glycoprotein endoplasmic reticulum-associated degradation and mannose trimming. J. Biol. Chem. *281*, 9650–9658.

8. Hosokawa, N., Tremblay, L.O., Sleno, B., Kamiya, Y., Wada, I., Nagata, K., Kato, K., and Herscovics, A. (2010). EDEM1 accelerates the trimming of alpha1,2-linked mannose on the C branch of N-glycans. Glycobiology *20*, 567–575.

9. Hosokawa, N., Tremblay, L.O., You, Z., Herscovics, A., Wada, I., and Nagata, K. (2003). Enhancement of endoplasmic reticulum (ER) degradation of misfolded Null Hong Kong alpha1-antitrypsin by human ER mannosidase I. J. Biol. Chem. *278*, 26287–26294.

10. Mast, S.W., Diekman, K., Karaveg, K., Davis, A., Sifers, R.N., and Moremen, K.W. (2005). Human EDEM2, a novel homolog of family 47 glycosidases, is involved in ER-associated degradation of glycoproteins. Glycobiology *15*, 421–436.

11. Ninagawa, S., Okada, T., Sumitomo, Y., Kamiya, Y., Kato, K., Horimoto, S., Ishikawa, T., Takeda, S., Sakuma, T., Yamamoto, T., et al. (2014). EDEM2 initiates mammalian glycoprotein ERAD by catalyzing the first mannose trimming step. J. Cell Biol. *206*, 347–356.

12. Olivari, S., Cali, T., Salo, K.E.H., Paganetti, P., Ruddock, L.W., and Molinari, M. (2006). EDEM1 regulates ER-associated degradation by accelerating de-mannosylation of folding-defective polypeptides and by inhibiting their covalent aggregation. Biochem. Biophys. Res. Commun. *349*, 1278–1284.

13. Hosokawa, N., Kamiya, Y., Kamiya, D., Kato, K., and Nagata, K. (2009). Human OS-9, a lectin required for glycoprotein endoplasmic reticulum-associated degradation, recognizes mannose-trimmed N-glycans. J. Biol. Chem. *284*, 17061–17068.

14. Fujita, E., Kouroku, Y., Isoai, A., Kumagai, H., Misutani, A., Matsuda, C., Hayashi, Y.K., and Momoi, T. (2007). Two endoplasmic reticulum-associated degradation (ERAD) systems

for the novel variant of the mutant dysferlin: ubiquitin/proteasome ERAD(I) and autophagy/lysosome ERAD(II). Hum. Mol. Genet. *16*, 618–629.

15. Hirsch, C., Gauss, R., Horn, S.C., Neuber, O., and Sommer, T. (2009). The ubiquitylation machinery of the endoplasmic reticulum. Nature *458*, 453–460.

16. Rashid, H.-O., Yadav, R.K., Kim, H.-R., and Chae, H.-J. (2015). ER stress: Autophagy induction, inhibition and selection. Autophagy *11*, 1956–1977.

17. Guerriero, C.J., and Brodsky, J.L. (2012). The delicate balance between secreted protein folding and endoplasmic reticulum-associated degradation in human physiology. Physiol. Rev. *92*, 537–576.

18. Shang, J., Körner, C., Freeze, H., and Lehrman, M.A. (2002). Extension of lipid-linked oligosaccharides is a high-priority aspect of the unfolded protein response: endoplasmic reticulum stress in Type I congenital disorder of glycosylation fibroblasts. Glycobiology *12*, 307–317.

19. Lecca, M.R., Wagner, U., Patrignani, A., Berger, E.G., and Hennet, T. (2005). Genome-wide analysis of the unfolded protein response in fibroblasts from congenital disorders of glycosylation type-I patients. FASEB J. Off. Publ. Fed. Am. Soc. Exp. Biol. *19*, 240–242.

20. Yuste-Checa, P., Vega, A.I., Martín-Higueras, C., Medrano, C., Gámez, A., Desviat, L.R., Ugarte, M., Pérez-Cerdá, C., and Pérez, B. (2017). DPAGT1-CDG: Functional analysis of disease-causing pathogenic mutations and role of endoplasmic reticulum stress. PloS One *12*, e0179456.

21. Walter, P., and Ron, D. (2011). The unfolded protein response: from stress pathway to homeostatic regulation. Science *334*, 1081–1086.

22. Ron, D., and Walter, P. (2007). Signal integration in the endoplasmic reticulum unfolded protein response. Nat. Rev. Mol. Cell Biol. *8*, 519–529.

23. Kim, I., Xu, W., and Reed, J.C. (2008). Cell death and endoplasmic reticulum stress: disease relevance and therapeutic opportunities. Nat. Rev. Drug Discov. *7*, 1013–1030.

24. Kimata, Y., and Kohno, K. (2011). Endoplasmic reticulum stress-sensing mechanisms in yeast and mammalian cells. Curr. Opin. Cell Biol. *23*, 135–142.

25. Termine, D.J., Moremen, K.W., and Sifers, R.N. (2009). The mammalian UPR boosts glycoprotein ERAD by suppressing the proteolytic downregulation of ER mannosidase I. J. Cell Sci. *122*, 976–984.

26. Xiang, C., Wang, Y., Zhang, H., and Han, F. (2017). The role of endoplasmic reticulum stress in neurodegenerative disease. Apoptosis Int. J. Program. Cell Death *22*, 1–26.

27. Fribley, A., Zhang, K., and Kaufman, R.J. (2009). Regulation of apoptosis by the unfolded protein response. Methods Mol. Biol. Clifton NJ *559*, 191–204.

28. Sano, R., and Reed, J.C. (2013). ER stress-induced cell death mechanisms. Biochim. Biophys. Acta BBA - Mol. Cell Res. *1833*, 3460–3470.

29. Tabas, I., and Ron, D. (2011). Integrating the mechanisms of apoptosis induced by endoplasmic reticulum stress. Nat. Cell Biol. *13*, 184–190.

30. Sobreira, N., Schiettecatte, F., Valle, D., and Hamosh, A. (2015). GeneMatcher: A Matching Tool for Connecting Investigators with an Interest in the Same Gene. Hum. Mutat. *36*, 928–930.

31. Schwarz, J.M., Cooper, D.N., Schuelke, M., and Seelow, D. (2014). MutationTaster2: mutation prediction for the deep-sequencing age. Nat. Methods *11*, 361–362.

32. Sim, N.-L., Kumar, P., Hu, J., Henikoff, S., Schneider, G., and Ng, P.C. (2012). SIFT web server: predicting effects of amino acid substitutions on proteins. Nucleic Acids Res. *40*, W452–W457.

33. Maquat, L.E. (1995). When cells stop making sense: effects of nonsense codons on RNA metabolism in vertebrate cells. RNA N. Y. N *1*, 453–465.

34. Baker, K.E., and Parker, R. (2004). Nonsense-mediated mRNA decay: terminating erroneous gene expression. Curr Opin Cell Biol *16*, 293–299.

35. Shenkman, M., Ron, E., Yehuda, R., Benyair, R., Khalaila, I., and Lederkremer, G.Z. (2018). Mannosidase activity of EDEM1 and EDEM2 depends on an unfolded state of their glycoprotein substrates. Commun. Biol. *1*, 172.

36. Chen, J., Li, X., Edmondson, A., Meyers, G.D., Izumi, K., Ackermann, A.M., Morava, E., Ficicioglu, C., Bennett, M.J., and He, M. (2019). Increased Clinical Sensitivity and Specificity of Plasma Protein N-Glycan Profiling for Diagnosing Congenital Disorders of Glycosylation by Use of Flow Injection-Electrospray Ionization-Quadrupole Time-of-Flight Mass Spectrometry. Clin. Chem. *65*, 653–663.

37. Zhang, W., James, P.M., Ng, B.G., Li, X., Xia, B., Rong, J., Asif, G., Raymond, K., Jones, M.A., Hegde, M., et al. (2016). A Novel N-Tetrasaccharide in Patients with Congenital Disorders of Glycosylation, Including Asparagine-Linked Glycosylation Protein 1, Phosphomannomutase 2, and Mannose Phosphate Isomerase Deficiencies. Clin. Chem. *62*, 208–217.

38. Davis, K., Webster, D., Smith, C., Jackson, S., Sinasac, D., Seargeant, L., Wei, X.-C., Ferreira, P., Midgley, J., Foster, Y., et al. (2017). ALG9-CDG: New clinical case and review of the literature. Mol. Genet. Metab. Rep. *13*, 55–63.

39. Foulquier, F., Duvet, S., Klein, A., Mir, A.-M., Chirat, F., and Cacan, R. (2004). Endoplasmic reticulum-associated degradation of glycoproteins bearing Man5GlcNAc2 and Man9GlcNAc2 species in the MI8-5 CHO cell line. Eur. J. Biochem. *271*, 398–404.